Full-Scale Experimental Testing on a Reinforced Bridge RC Beam: Experimental and SHM Results

Full-scale experimental testing on a reinforced bridge RC beam: experimental and SHM results

P. Darò[1*][0000-0001-5805-216X], D. La Mazza[1][0000-0001-8255-3933], E. Tetta[1], G. Lastrico[1], I. Alovisi[1], G. Mancini[1,2], E. Miceli[2][0000-0002-1262-3403], D. Gino[2][0000-0002-8689-0790], G. Amendola[2][0000-0002-1262-3403], L. Giordano[2][0000-0003-2006-9438], P. Castaldo[2][0000-0002-7956-9392], M. Mariscotti[3], M. Garozzo[3], M. Deiana[4], B. Magrì[4]

[1*]Sacertis Ingegneria S.r.l.,10126 Torino, Italy, corresponding author
paola.daro@sacertis.com
[2] Dipartimento di Ingegneria Strutturale, Edile e Geotecnica (DISEG), Politecnico di Torino, Corso Duca degli Abruzzi 24, Turin 10129
[3] Sina S.p.A
[4] Autostrada dei Fiori S.p.A

Abstract. Asset managers, owners and the engineering companies are facing the increasing need to accurately estimate the actual structural condition of existing infrastructures as well as assess their residual life with respect to predetermined reliability levels. In this context, existing concrete bridges require special attention due to the growing progressive ageing, deterioration mechanisms as well as the increased traffic loads, coupled with the reach of the nominal reference life. To this extent, a full-scale experimental testing campaign has been carried out on a reinforced concrete simply supported beam built around 55 years ago and with a span equal to 25.90m. The reinforced concrete (RC) beam was removed during the demolition operations of the Mollere viaduct, along the A6 highway, in Italy. The testing campaign consisted of a load-controlled test where the beam, supported on isolated foundations, has been directly loaded with a system of cast iron masses calibrated to reach the near-collapse state at the end of the test. The beam has been instrumented with continuous monitoring systems to effectively observe its structural behaviour throughout the experimental test. This paper summarizes the load test setting and the main results in terms of both the static behaviour, showing the efficiency of the testing campaign as well the accuracy of the monitoring systems applied.

Keywords: *concrete bridges, full-scale testing, RC beam, SHM*

1 Introduction

In the last few years, asset managers, owners and the engineering companies are facing the increasing need to estimate the actual structural condition of existing infrastructures as well as assess their residual working life with respect to predetermined reliability levels [1]-[4]. In fact, the evaluation of the structural safety of existing bridges is extremely relevant for companies that manages large-scale infrastructures.

In detail, it is of interest to investigate actual behavior of existing bridges with the aim to plan interventions, maintenance and even monitoring programs in agreement with the evolution of design codes in both National and International field [5]-[8]. In this context, existing reinforced and prestressed concrete bridges require special attention due to the ageing and deterioration mechanisms as well as the increased magnitude of traffic loads [9]. In the past, full-scale experimental tests on existing reinforced concrete (RC) and prestressed concrete (PC) beams which have overpassed their intended working life have been successfully performed [10]. However, to plan full-scale tests on dismantled existing bridges beams is generally complex for what concerns costs, logistic and development of suitable testing procedures and devices.

In this investigation, a full-scale experimental testing campaign on a RC bridge beam built more than 60 years ago is presented. The bridge beam is simply supported and have a span equal to 25.90m. The RC beam was removed during the demolition operations of the Mollere viaduct, along the A6 highway, in Italy. The testing campaign consisted of a load-controlled test where the beam, supported on isolated foundations, has been directly loaded with a system of cast iron masses calibrated to reach the near-collapse state at the end of the test. The beam has been instrumented with continuous monitoring systems to effectively observe the structural behaviour of the beam throughout the experimental test. The present work illustrates the set up for the realization of the full-scale test and the main results in terms of static behavior. In particular, the results are useful to discuss and demonstrate the efficiency of the testing campaign as well the accuracy of the monitoring systems.

2 Description of the RC bridge beam and data available before testing

The beam selected for the full-scale load test presented in this paper is a simply supported reinforced concrete beam having a 25.90m span. The RC beam has been dismantled from the Mollere viaduct, along the A6 highway in Italy, after around 55 years of working life. The main features related to the geometry are reported in Figure 1(a-b). In detail, the beam has been dismantled from a girder bridge deck composed of 6 RC precasted RC beams having overall height of 185 cm with 20cm thick cast in-situ reinforced concrete slab.

As shown in Figure 1(a), the edge beam has been selected for the test, as it was the most damaged one due to its increased exposition to environmental actions and water leakage from the platform. As a result of the required operations for the execution of the longitudinal cut during the dismantling operations, the RC beam is characterized by an asymmetrical cross-section.

By means of the analysis of the historical documentation and on-field inspections, the main features of the materials used to build the RC beam have been identified. In particular, the beam presents main reinforcement for bending composed by 20 ϕ28 longitudinal bars (Figure 1(c)). These bars are bent in correspondence of the edges of the beam with the aim to bear the major part of the shear force inside the web.

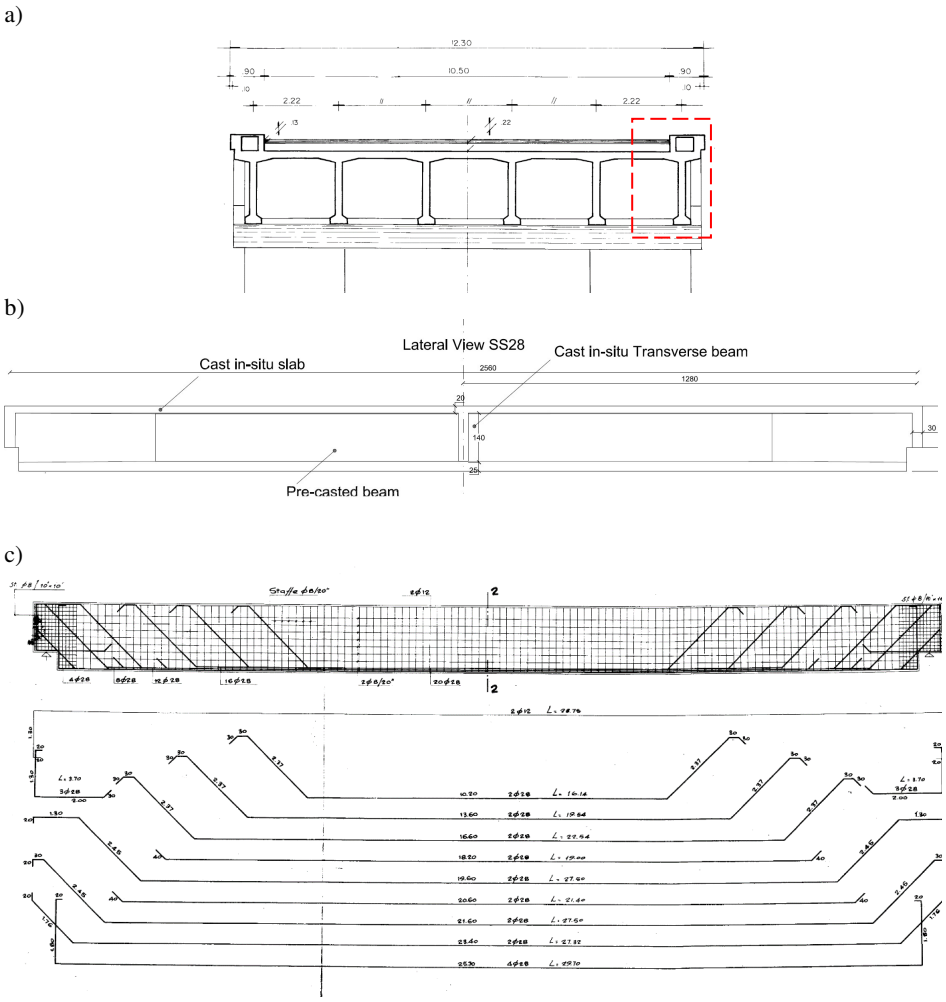

Fig. 1. Main features of the RC bridge beam of the Mollere viaduct: a) cross section of the deck and selected edge beam (measures in m); b) lateral view of the beam after the longitudinal cut (measures in cm); c) detail of the main reinforcement of the precast RC beam.

In particular, the cast "in situ" concrete which composes the top RC slab presents cubic characteristic compressive strength (R_{ck}) equal to 24 MPa that corresponds to 20.75 MPa as for related cylinder one (f_{ck}). The mean value of the cylinder compressive strength (f_{cm}) can be assumed equal to 28.75 MPa [8]. The concrete that constitutes the RC precast beam have R_{ck} equal to 35 MPa which correspond to f_{ck} equal to 29.05 MPa. The related f_{cm} is equal to 37.05 MPa [8]. The steel reinforcements are represented by ribbed bars having squared cross section with characteristic value of yielding strength (f_{yk}) equal to 440 MPa (FeB44k). The mean value f_{ym} can be estimated as 484 MPa [8]. The elastic modulus is assumed equal to 200000 MPa. All the

material properties not available from historical documentation have been assumed according to [8],[11].

3 Structural health monitoring and static testing procedure

In this section the test configuration and procedure together with the monitoring systems adopted are described.

3.1 Test procedure and set-up

The test set-up consisted in the application of a vertical static load by means of iron masses (i.e., iron pallets), each having a weight of 105 kN and dimensions of 35 cm height, 243 cm width and 194 cm depth. In particular, the midspan of the beam was loaded over a length of about 11 m along its axis, by aligning four iron pallets (Figure 3). In order to reduce, as much as possible, the torsional rotations around the longitudinal axis, two symmetric steel supports were placed, each of them at a distance of 275 cm from the midspan. Two hydraulic jacks supported by layers of Azobé wood were placed below each of these torsional supports. An additional supporting system was placed below the beam in correspondence of the central area, made of a steel plate 5 cm thick, placed on top of four hydraulic jacks, which were supported by layers of Azobé wood. It is noteworthy that the steel plate was not in contact with the beam but was kept at a distance of a few centimeters from the intrados of the beam, as a measure of safety in case of an eventual occurrence of a brittle failure.

By considering the mean values of the mechanical properties of the materials, a resisting flexural moment of 10728 kNm was computed. With the goal to reach this estimated ultimate resistance, it was decided to load the structure with 4 different layers (i.e., SA, SB, SC, SD), each of them made of 4 iron weights (i.e., 1, 2, 3 and 4) placed over a width of 11 m in correspondence of the midspan. Since each layer of iron pallets weights 420 kN, by summing up the 4 layers, a total load of 1680 kN was provided.

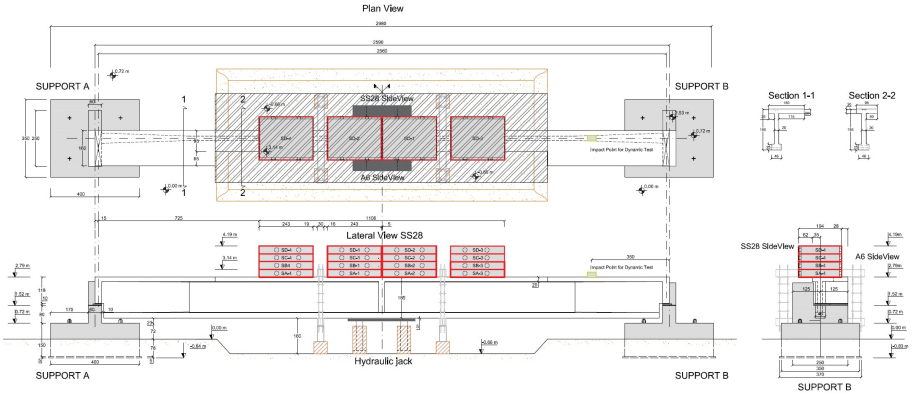

Fig. 3. Experimental test set-up.

Figure 4(a-b) illustrates the different stages of load application before failure occurred and the picture representing the loading operations. The first and the second stages are equal and consisted in the application of four steps of load (such that the layer SA was placed), followed by four steps of unload. The third stage consisted in the loading of two layers of iron pallets (i.e., layer SA and SB) followed by their unloading and the last stage ended with the application of three layers of iron pallets (i.e., layer SA, SB and SC). Hence, collapse occurred in correspondence of a total load of 1260 kN, which coincided with the positioning of the SC1-4 iron weight. The observed collapse mechanism consists of a bi-axial bending failure mode due to the failure of the top slab concrete placed in proximity of the midspan. It should be evidenced that the top slab in the 90ties was repaired with demolition of the top layer for few centimeters and reinforced with additional high strength concrete not mechanically connected to the original one. As a consequence, at failure the additional concrete layer was detached from the beam causing a brittle mechanism.

a)

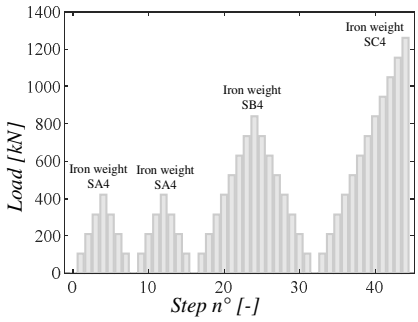

b)

Fig. 4. Experimental test procedure: a) number of loading steps and applied load; b) picture of the loading operations and of the test-set configuration.

3.2 Description of the adopted SHM system

Among the variety of sensors installed to record the site load test, the present paper focuses on the analysis of the static response registered by the SHM (i.e., Structural Health Monitoring) continuous monitoring systems installed and processed by Sacertis Ingegneria S.r.l. The RC beam was instrumented with 5 MEMS (i.e., Micro Electro-Mechanical System) bi-axial clinometers and 5 tri-axial accelerometers, wired connected using a power-line based architecture combined with a CAN-BUS network to a IoT Gateway installed near one of the plinths. In terms of positioning along the beam, sensors are placed close to both the span ends (Sens. T1.1.1. and T1.1.5) and at about 1/3 (T1.1.2), 1/2 (T1.1.3) and 3/4 (T1.1.4) of the span length, as shown in Figure 4.

The data gathered from the sensors have been filtered at the gateway level and sent to both a local server for near-real time processing as well as to the Cloud for data storage and further post-processing. The bi-axial MEMS clinometers, analyzed in

the present paper, provide rotations around axes x and y in the horizontal plane. Specifically, the x axis corresponds to the transversal direction of the beam (torsional behaviour), whilst the y axis is parallel to the longitudinal direction of the beam (flexural behaviour).

MEMS clinometers have a 32-bit microcontroller and are provided with humidity and temperature sensors installed inside the sensor node box. The clinometer data are collected in sequential samples, averaged over a 1s window with a sampling frequency of 208 Hz, providing synthetic statistical parameters like the mean value, standard deviation, maximum and minimum rotation, internal temperature, and relative humidity.

MEMS bi-axial clinometers allow to monitor the evolution in time of the local rotations under progressive load as well as after the unloading processes as plastic residual rotations arise as a consequence of the damage process [12][13]. The static response derived from the analysis of the MEMS sensors is compared with the topographic monitoring of the vertical displacements, registered under sensors T1.1.3 at midspan and T1.1.4 at 3/4L.

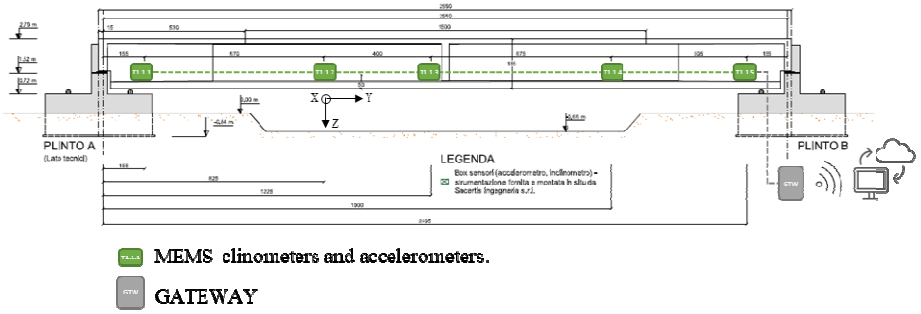

Fig. 4. MEMS clinometers and accelerometers monitoring system.

4 Experimental results

As regards the static response, Figure 5a shows the load-displacement curve derived from the MEMS clinometers with respect to the deflection at mid-span, compared with the recordings or the topographic monitoring. The results are presented following the i-th progressively increasing load phase (from 1 to 4) described in Section 3.1. It can be noticed from Figure 5a that there is a very good correspondence in terms of direct (topographic monitoring) and indirect measurement (deformed shape derived from MEMS clinometers installed at discrete locations along the beam) of the mid-span displacement.

Figure 5b illustrates the trend over time of the rotations read by the clinometer sensors T1.1.4, installed at 3/4L, in the y direction (longitudinal axis of the beam), representative of the bending of the beam in the vertical plane. Due to the short-term duration of site test performed, no thermal compensation of the signal has been re-

quired due to the limited environmental condition influence on the structural response and on the sensors.

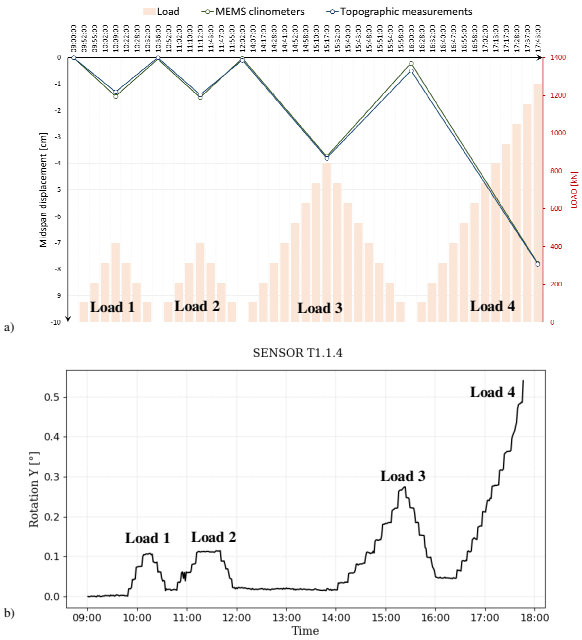

Fig. 5. Experimental results: a) Load-displacement curve derived from the MEMS clinometers analysis, compared with the topographic monitoring at mid-span; b) Evolution of the flexural rotation registered by sensor T1.1.4 installed at 3/4L.

It can be noticed that for the first two loading and unloading cycles up to 420kN, the RC beam responds in a linear-elastic condition, there is a symmetry in the rotations and therefore in the deformation of the beam under load, with limited evidence of a residual rotation induced by local damages read by sensor T1.1.4. Following the third loading-unloading cycle, up to 840kN, a considerable residual rotation equal to 0.05° is detected by the sensor T1.1.4, which corresponds to the formation of a cracking pattern concentrated near the measuring point, and subsequently subjected to control with an LVDT sensor, as shown in Figure 6. The deformation assumes an asymmetrical trend in load step 4, up to collapse. The load-displacement curve as well as the recorded rotations indicate a lack of plasticization of the beam, except for the final phase before the collapse. In the x transverse direction, on the other hand, the rotations of the clinometer sensors confirmed the progressive accumulation of a rigid rotation around the longitudinal axis of the beam, equal in sign for all the sensors, during the entire course of the test. These rotations were never fully recovered in the unloading phase and reasonably reached their maximum value in the instant preceding the overturning of the beam itself.

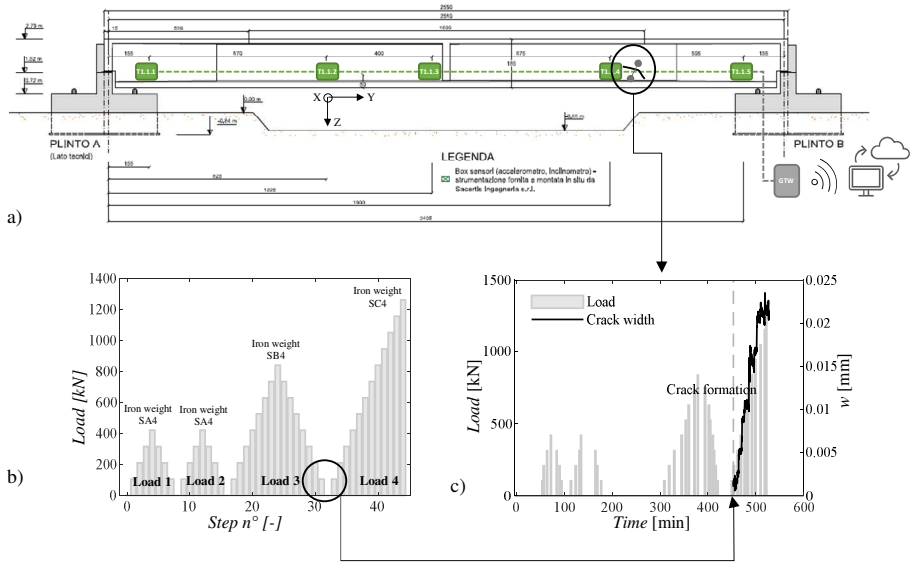

Cracking evidence near T1.1.4 between Unload 3 and Load 4

Fig. 6. a) Location of the cracking formed after Load 3; b) Crack width in mm measured with horizontal LVDT vs Time [min].

Figure 7a presents the deformed shape derived from the MEMS clinometers under Load steps 1, 2, 3 and 4, compared to the measurements of the topographic sensors installed at L/2 (Sensor P9) and installed at 3/4L (Sensor P7). There is an accurate correspondence and cross-correlation between both the direct and indirect measurements performed by the different types of instruments installed to support the diagnostic activities and the identification of the main damage mechanisms.

Figure 7b shows the residual deformed shape after each i-th unloading step. It can be noticed that up to Load 2, the deformed shape under 420kN remains almost symmetric and limited sign of residual rotation is recorded. The residual deflections after load steps 1 and 2 are comparable and are affected by the adjustments made to the support conditions during the first phases of the site test. The deflected shape under Load 3 (860kN) shows the asymmetry induced by the local damage occurred near sensor T1.1.4 (3/4 L); the asymmetry and concentrated rotation became even more evident under Load 4, recorded just before the beam collapse. A residual rotation concentrated at 3/4 of the span induced an asymmetric residual deflection equal to 2mm. Therefore, the analysis of the reference parameters of the structural response (such as rotations under load and residual, displacements and deformations, crack opening,..) proved to be good indicators of the variation of response as the application of the load proceeded, accurately representing the effect of the variable constraint conditions and progress of the damage.

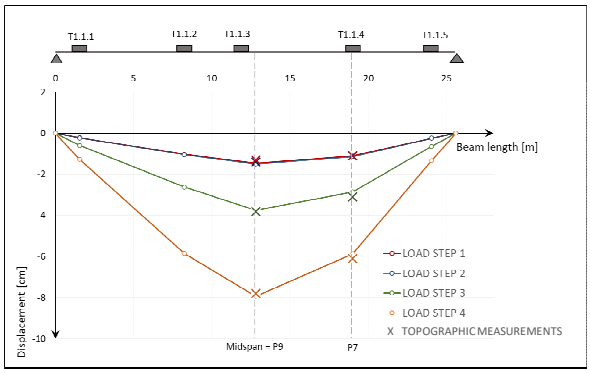

a)

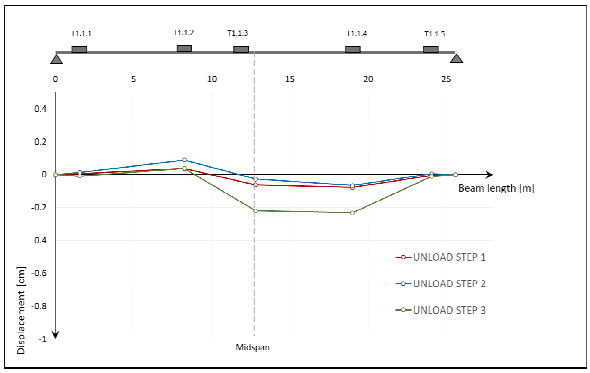

b)

Fig. 7. a) Deformed shape derived from the MEMS clinometers under Load steps 1, 2, 3 and 4; b) Deformed shape derived from the MEMS clinometers after the unloading phase at steps 1, 2, 3, showing the effect of the local damages and residual rotations.

5 Conclusions

This paper proposes and illustrates some of the achievements related to the full-scale experimental testing of an existing RC bridge beam after around 60 years of working life. The selected beam presents very common features with respect to a major part of the beams used during the ‘60s to build highways girder bridges in Italy. In particular, after the description of the beam selected for the test and of the related testing procedure, the main outcomes derived from the SHM system provided by Sacertis Ingegneria S.r.l. in terms of static response are reported and compared to other direct measurement systems (topographic monitoring), showing a good cross-correlation. As widely recognised, the use of SHM systems with continuous data acquisition are becoming of high interest for infrastructures managers. The RC bridge beam was instrumented with 5 MEMS bi-axial clinometers and 5 tri-axial accelerometers appropriately located along the beam span. The results of the test and of the related monitoring are of high relevance because they allow to assess the performances of the mentioned above SHM system over the loading and damaging process of the beam. In particular, the SHM devices were able to catch the non-symmetric static response of the beam approaching the failure condition. The analysis of the results is useful to increase the ability of professionals and engineers to interpret

the observed data from SHM installed on bridges along main infrastructures. For instance, further research is ongoing with the aim to propose methodologies able to determine safety thresholds of the monitored parameters at the purpose of prompt intervention by the Authorities in case of adverse events.

References

1. Miluccio, G., Losanno, D., Parisi, F., and Cosenza, E. 2021. "Traffic-load fragility models for prestressed concrete girder decks of existing Italian highway bridges." Engineering Structures, 249, 113367.
2. Santarsiero, G.; Masi, A.; Picciano, V.; Digrisolo, A. The Italian Guidelines on Risk Classification and Management of Bridges: Applications and Remarks on Large Scale Risk Assessments. Infrastructures 2021, 6, 111. https://doi.org/10.3390/infrastructures6080111
3. Cardone, D., Giuseppe, P. and Salvatore, S. 2011. "A performance-based adaptive methodology for the seismic evaluation of multi-span simply supported deck bridges. " Bull Earthq Eng , 9(5):1463–98.
4. Castaldo, P., Gino, D., Marano, G.C. and Mancini, G. 2022. "Aleatory uncertainties with global resistance safety factors for non-linear analyses of slender reinforced concrete columns." Engineering Structures, 255, 113920
5. Linee guida per la classificazione e gestione del rischio, la valutazione della sicurezza ed il monitoraggio dei ponti esistenti. Italian High Council of Public Works, Rome, Italy, 2020 (in Italian).
6. DM 17/12/2020, n. 578. Adozione delle linee guida per la gestione del rischio dei ponti esistenti e per la definizione di requisiti ed indicazioni relativi al sistema di monitoraggio dinamico. Italian Ministry of Infrastructures and Transportation, Rome, Italy, 2020 (in Italian).
7. DM 17/01/2018. Aggiornamento delle "Norme tecniche per le costruzioni". Italian Ministry of Infrastructures and Transportation, Rome, Italy, 2018 (in Italian).
8. CEN. EN 1992-1-1. Eurocode 2: Design of concrete structures – Part 1-1: General rules and rules for buildings. Brussels, Belgium: Comite Europeen de Normalisation; 2004.
9. Bagge N. Demonstration and examination of a procedure for successively improved structural assessment of concrete bridges. Structural Concrete. 2019;1–24.
10. Botte W, Vereecken E, Taerwe L, Caspeele R. Assessment of posttensioned concrete beams from the 1940s: Large-scale load testing, numerical analysis and Bayesian assessment of prestressing losses. Structural Concrete. 2021;1–23. https://doi.org/10.1002/suco.202000774
11. fib Model Code for Concrete Structures 2010. fib 2013. Lausanne.
12. Alovisi, I. *et al.* (2022). New Sensor Nodes, Cloud, and Data Analytics: Case Studies on Large Scale SHM Systems. In: Cury, A., Ribeiro, D., Ubertini, F., Todd, M.D. (eds) Structural Health Monitoring Based on Data Science Techniques. Structural Integrity, vol 21. Springer, Cham. https://doi.org/10.1007/978-3-030-81716-9_22
13. Basone, F., Cigada, A., Darò, P., Lastrico, G., Longo, M., Mancini, G. (2023). Concrete Bridges Continuous SHM Using MEMS Sensors: Anomaly Detection for Preventive Maintenance. In: Rizzo, P., Milazzo, A. (eds) European Workshop on Structural Health Monitoring. EWSHM 2022. Lecture Notes in Civil Engineering, vol 253. Springer, Cham. https://doi.org/10.1007/978-3-031-07254-3_47